Printability of carboxymethyl cellulose/glass-containing inks for robocasting deposition in reversible solid oxide cell applications

Soukaina Lamnini [a], Francesco Baino [a], Giorgia Montalbano [a], Hassan Javed [b], Federico Smeacetto [a,*]

[a] Department of Applied Science and Technology, Politecnico di Torino, Turin, Italy
[b] Sunfire GmbH, Dresden, Germany

ARTICLE INFO

ABSTRACT

Water-based inks containing carboxymethyl cellulose (CMC) and glass particles were investigated in terms of rheological properties and printability for solid oxide cell joining application using robocasting for the first time. The ink formulation containing 36 vol% of glass showed the highest yield stress (9.6×10^2 Pa) and viscosity (4×10^4 Pa·s). CMC-based paste with 37 vol% of glass was selected for printing on Crofer22APU steel substrate due to its relatively low viscosity (2.6×10^4 Pa·s) and high storage modulus (1.4×10^5 Pa), thus ensuring an easier extrusion and shape retention upon printing. The high solid loading of 37 vol% along with optimised debinding and sintering stages enabled achieving high-quality Crofer22APU/glass sealant joining with a reproducible thickness and low porosity.

1. Introduction

Solid oxide cells (SOCs) can efficiently operate as either electrolysis cells or fuel cells [1–3]. In order to avoid gas leakage and fuel-oxidant mixing, sealants for SOCs should fulfil several requirements, including hermeticity, high thermal/chemical stability, and excellent interfacial compatibility with neighbouring components [4,5]. In this regard, glasses and glass-ceramics proved to be suitable in the manufacturing of SOCs to bond multiple unit cells connected by metallic interconnects, such as Crofer22APU and AISI441 [2,4,6]. The needs for applying glass sealants on complex geometries and ensuring a controllable thickness and homogeneity of the sealant along the surface to be sealed are additional goals that, however, are hard to be reached by conventional manufacturing methods, which also allow limited scalability towards industrial mass-production.

Additive manufacturing technologies (AMTs) can successfully overcome many of the limitations mentioned above since complex shapes can be obtained with high accuracy over the predefined architecture, repeatability and great potential to process automation [7,8]. Among AMTs, robocasting involves the direct extrusion of high-solid-loading suspensions to build products via layer-wise deposition [9]. An ink with suitable rheological properties for printing should be able to flow through the extrusion nozzle and exhibit good shape retention capacity upon deposition [10]. Glass-based inks are typically prepared by adding the inorganic powder to a solvent using an anionic polyelectrolyte in order to obtain a concentrated slurry; then, a temperature-, pH- or salt-induced rheological change allows turning the suspension into a gel-like system [11,12].

The need for extending the printability window of the ink and fine-tuning the physico-mechanical properties often led researchers towards the design of multicomponent ink formulations carrying additional complexity to the system. In the present work, carboxymethyl cellulose (CMC) is proposed as a single multifunctional additive with both dispersing and binding functions in order to formulate a water-based paste. A similar approach was suggested by Eqtesadi et al. [13] to fabricate 45S5 Bioglass® scaffolds for regenerative medicine but has not been reported in the field of SOCs so far.

2. Materials and methods

2.1. Materials and ink preparation

A silica-based, B-containing glass–ceramic sealant with composition and properties similar to those reported in [14] was used as feedstock to charge the inks. Inks were prepared by dissolving 3 wt% of CMC (Sigma Aldrich) in deionized water for 5 h under magnetic stirring to form a

---

* Corresponding author.
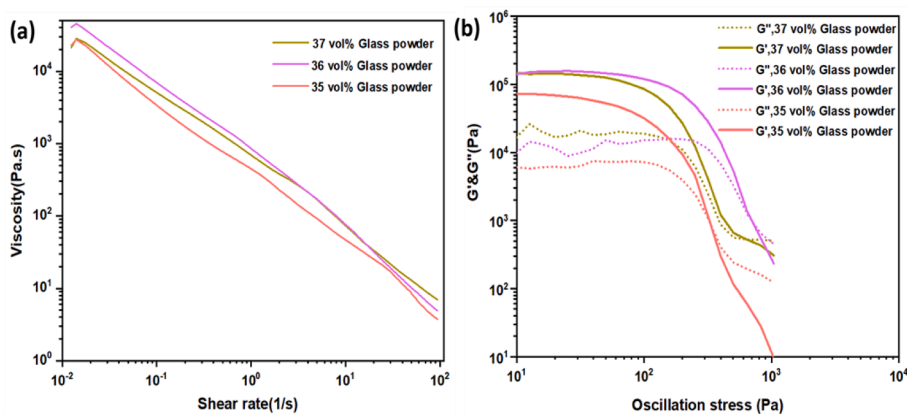 *E-mail address:* federico.smeacetto@polito.it (F. Smeacetto).

Fig. 1. Viscoelastic properties of inks containing 35, 36 and 37 vol% of glass: (a) flow ramp and (b) oscillatory amplitude sweep test.

homogeneous solution. Then, glass powders (35, 36 or 37 vol%; $D_{50} \sim$ 40 µm) were added to the CMC solution batches that were mixed in a centrifugal planetary mixer according to the optimised multistep process (4 cycles at 700 rpm for 3 min each followed by 4 cycles at 1200 rpm for 2 min each; cooling for 1 min in ice bath after each cycle; final centrifugation at 1200 rpm for 3 min). The inks were stored in the fridge for 1 h prior to printing at room temperature.

2.2. Robocasting and thermal treatment

Each ink was housed in a polypropylene syringe and extruded through conical nozzles with different inner diameters (4 mm, 2 mm, 500 µm,104 µm) by the computer-controlled robotic system (Z-Morph Fab) following the CAD model. Ink combining both good viscoelastic behaviour and high packing density was chosen for printing with a tip of 500 µm. The printing substrate to form the joining was a 30 mm × 30 mm Crofer22APU square plate. Printing, piston and retraction speeds were adjusted upon ink viscosity and stiffness results to 10 mm/s, 10 mm/s, 40 mm/s respectively, while the tip-to-substrate distance was fixed at 0.5 mm. Printed layers with square-shaped geometry were adapted to Crofer22APU substrate dimensions; the printed area did not cover all the plate surface. The printed products underwent homogenous drying in ambient air for 24 h to reduce drying-induced stresses. Based on thermal analysis results, debinding and sintering stages (performed in air inside a furnace) were carried out at 400 °C/1h and 930 °C/1h, respectively (heating rate 2 °C/min in both cases). Samples were finally cooled down to room temperature at 2 °C/min.

2.3. Characterizations

The thermal behaviour of dried ink was studied by means of differential thermal analysis (DTA; Netzsch 404PC) and hot-stage microscopy (HSM; Hesse Heating Microscope) in air from room temperature to 1000 °C at 5 °C/min heating and cooling rates.

The rheological properties of the inks were assessed using a DHR-2 controlled stress rotational rheometer (TA Instruments, Waters, USA) equipped with a parallel plate geometry (diameter 20 mm) and a Peltier plate system to constantly control the temperature. All the tests were performed at room temperature similarly to the printing environment. Flow ramp tests (n = 3) were carried out to investigate the variation of inks viscosity over a wide range of shear rates (0.01–1000 s^{-1}). Amplitude sweep tests (n = 3) were performed by applying oscillation stresses (10^1–10^3 Pa) at 1 Hz to monitor the viscoelastic properties of the inks. Morphology of joined samples was investigated by scanning electron microscopy (JCM 6000Plus Versatile Benchtop SEM, JEOL).

Table 1
Rheological properties of glass inks.

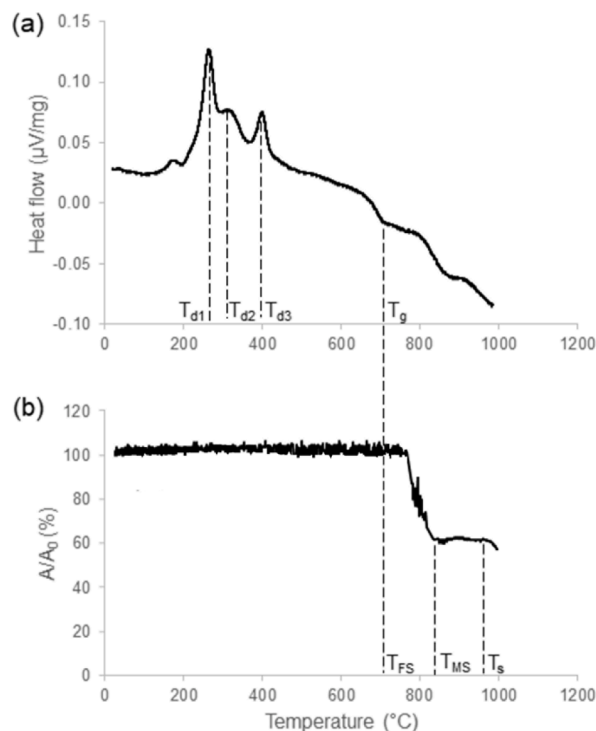| Solid loading (vol. %)	Viscosity, η (Pa·s)	Storage modulus, G′ (Pa)	Yield stress, τ_y (Pa)
35	2.6×10^4	7.4×10^4	3.2×10^2
36	4.0×10^4	1.4×10^5	9.6×10^2
37	2.6×10^4	1.4×10^5	5.2×10^2

Fig. 2. Thermal analyses of dried ink (37 vol% of glass): (a) DTA and (b) HSM (A/A_0 = actual area/initial area).

3. Results and discussion

Fig. 1a shows the viscosity (η) variation as a function of shear rate. Regardless of glass loading, all inks present a shear-thinning behaviour characterized by an exponential decrease of viscosity at increasing shear rates. This shear-thinning behaviour is a key requirement for ink printability and extrudability through fine tips. At the lowest shear rate of 0.01 s^{-1}, η is relatively high with 36 vol% compared to 35 and 37 vol
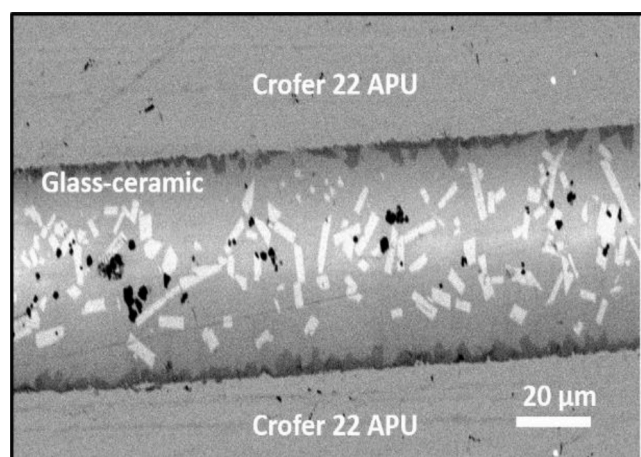
Fig. 3. SEM micrograph of the sintered Crofer22APU/glass/Crofer22-APU joining.

% glass loading. A practically inverse trend can be observed in the region of shear rates expected for printing (20–100 s^{-1}) considering inks containing 36 vol% and 37 vol% of glass, which is consistent with the literature [15–17]. The oscillatory amplitude sweep tests (Fig. 1b) revealed a wide linear viscoelastic region (LVR) and high yield stress (τ_y) values for all the inks indicated by the sudden drop of G' at shear stresses > 100 Pa, which corresponds to the solid–to–liquid-like transition and the disruption of the material networks. Larger concentrations of glass yielded higher G' and stiffness that, together with the large LVR ensure inks shape retention [10]. The rheogical properties of the inks are summarised in Table 1. Among others [16,17], powder loading is a key factor influencing directly the visco-elastic properties. Although ink containing 36 vol% presented superior stiffness, the ink with 37 vol% of glass was selected for joining because of high G' ensuring shape retention after extrusion, better printability and higher powder loading that is desirable to improve the density of sintered products.

Fig. 2 displays DTA and HSM results of as-dried ink containing 37 vol% of glass. The three exothermic peaks observed in Fig. 2a at T_{d1} ~264 °C, T_{d2} ~320 °C and T_{d3} ~398 °C correspond to thermal degradation of CMC occurring in three successive steps; this is consistent with previous findings by other authors [13]. HSM curve plotted in Fig. 2b shows that the printed material exhibits a clear densification step upon heating with maximum A/A$_0$ ~60%. Densification begins at T_{FS} (first shrinkage) occurs at around ~700 °C and continues till the maximum shrinkage is reached (T_{MS} ~850 °C). Applying appropriate debinding and sintering stages is key for the development of high-quality robocast glass and ceramic products: based on DTA and HSM results, CMC debinding was performed at 400 °C (~T_{d3}, complete burning-off of CMC) while the sintering temperature (T_s = 930 °C) was selected at the end of densification plateau.

A SEM micrograph of the Crofer22APU/glass/Crofer22APU cross-section is shown in Fig. 3. The glass-derived sealing exhibits a uniform and continuous thickness of ~ 52 μm, evidencing a homogeneous shrinkage due to drying/sintering effects and a minimal distortion of the printed layers due to either gravity or ink overflow. The solid loading of 37 vol% combined with the thermal treatment described above allow obtaining high-density sintered products with an almost pore-free microstructure. SEM micrograph also shows an outstanding interfacial bonding of the glass–ceramic to Crofer22APU (an oxide scale was formed onto the Crofer22APU due to sintering in air) without any traces of cracks or delamination, thereby confirming the good integrity of the sealant and the suitability of the selected sintering and debinding cycles.

4. Conclusions

This work focuses on developing a novel glass–ceramic sealing material for SOCs, combining robocasting and the use of CMC as a single multifunctional additive. Successful optimization and synthesis of inks containing glass loading of 35–37 vol% was experimentally demonstrated. The ink containing 37 vol% of glass was selected for printing and joining experiments. Outstanding interfacial bonding and remarkable thickness homogeneity of the Crofer22APU/glass/Crofer22APU joining was achieved, thus suggesting the potential of the developed printing and sintering processes for the deposition of glass sealants for SOC application.

The findings from this study will be of interest for an improved automation and processing of scalable stack components with the added value of applying water-based CMC/glass-containing ink formulations, thus avoiding the use of organic solvents and minimizing the amount of wastes in the whole process.

CRediT authorship contribution statement

Soukaina Lamnini: Writing – original draft, Investigation, Conceptualization, Data curation. **Francesco Baino:** Validation, Writing - review & editing. **Giorgia Montalbano:** Data curation, Investigation. **Hassan Javed:** Validation, Writing - review & editing. **Federico Smeacetto:** Funding acquisition, Supervision, Resources, Writing - review & editing.

Declaration of Competing Interest

The authors declare that they have no known competing financial interests or personal relationships that could have appeared to influence the work reported in this paper.

Acknowledgments

References

[1] F. Sartori da Silva, T.M. De Souza, Int. J. Hydrogen Energy 42 (2017) 26020–26036.
[2] F. Smeacetto, M. Salvo, M. Ferraris, J. Cho, A.R. Boccaccini, J. Eur. Ceram. Soc. 28 (2008) 61–68.
[3] H. Tu, U. Stimming, J. Power Sources 127 (2004) 284–293.
[4] H. Elsayed, H. Javed, A.G. Sabato, F. Smeacetto, E. Bernardo, J. Eur. Ceram. Soc. 38 (2018) 4245–4251.
[5] N. Mahato, A. Banerjee, A. Gupta, S. Omar, K. Balani, Prog. Mater. Sci. 72 (2015) 141–337.
[6] A.G. Sabato, G. Cempura, D. Montinaro, A. Chrysanthou, M. Salvo, E. Bernardo, M. Secco, F. Smeacetto, J. Power Sources 328 (2016) 262–270.
[7] E. Feilden, M.I. Factory, L. Vandeperre, J. Eur. Ceram. Soc. 36 (2016) 2525–2533.
[8] F. Baino, E. Fiume, Materials 13 (2020) 1688.
[9] J.A. Lewis, J.E. Smay, J. Stuecker, J. Cesarano III, J. Am. Ceram. Soc. 89 (2006) 3599–3609.
[10] J. Cesarano III, J.R. Segalman, P. Calvert, Ceram. Ind. 148 (1998) 94–102.
[11] P. Miranda, E. Saiz, K. Gryn, A.P. Tomsia, Acta Biomater. 2 (2006) 457–466.
[12] J. Barberi, F. Baino, E. Fiume, G. Orlygsson, A. Nommeots-Nomm, J. Massera, E. Verné, Materials 12 (2019) 2691.
[13] S. Eqtesadi, A. Motealleh, P. Miranda, A. Lemos, A. Rebelo, J.M.F. Ferreira, Mater. Lett. 93 (2013) 68–71.
[14] H. Javed, A.G. Sabato, M. Mansourkiaei, D. Ferrero, M. Santarelli, K. Herbrig, C. Walter, F. Smeacetto, Energies. 13 (2020) 3682.
[15] C.R. Tubío, F. Guitián, A. Gil, J. Eur. Ceram. Soc. 36 (2016) 3409–3415.
[16] A. Shahzad, I. Lazoglu, Compos. B Eng. 225 (2021), 109249.
[17] L. del-Mazo-Barbara, M.P. Ginebra, J. Eur. Ceram. Soc. 41 (2021) 18–33.